

Closed-loop model identification and PID/PI tuning for robust anti-slug control

Esmail Jahanshahi, Sigurd Skogestad¹

Department of Chemical Engineering, Norwegian Univ. of Science and
technology, Trondheim, NO-7491 (e-mail: skoge@ntnu.no).

Abstract: Active control of the production choke valve is the recommended solution to prevent severe slugging flow at offshore oilfields. This requires operation in an open-loop unstable operating point. It is possible to use PI or PID controllers which are the preferred choice in the industry, but they need to be tuned appropriately for robustness against plant changes and large inflow disturbances. The focus of this paper is on finding tuning rules based on model identification from a closed-loop step test. We perform an IMC (Internal Model Control) design based on the identified model, and from this we obtain PID and PI tuning parameters. In addition, we find simple PI tuning rules for the whole operation range of the system considering the nonlinearity of the static gain. The proposed model identification and tuning rules show applicability and robustness in experiments on a test rigs as well as in simulations using the OLGA simulator.

Keywords: Oil production, anti-slug control, unstable systems, robust control

1. INTRODUCTION

The severe-slugging flow regime at offshore oilfields is characterized by large oscillatory variations in pressure and flow rates. This flow regime in multi-phase pipelines and risers is undesirable and an effective solution is needed to suppress it (Godhavn et al. (2005)). One way to prevent this behaviour is to reduce the opening of the top-side choke valve. However, this conventional solution increases the back pressure of the valve, and it reduces the production rate from the oil wells. The recommended solution to maintain a non-oscillatory flow regime together with the maximum possible production rate is active control of the topside choke valve (Havre et al. (2000)). Measurements such as pressure, flow rate or fluid density are used as the controlled variables and the topside choke valve is the main manipulated variable.

Existing anti-slug control systems are not robust and tend to become unstable after some time, because of inflow disturbances or plant changes. The main objective of our research is to find a robust solution for anti-slug control systems. The nonlinearity at different operating conditions is one source of plant change, because gain of the system changes drastically for different operating conditions. In addition, the time delay is another problematic factor for stabilization.

One solution is to use nonlinear model-based controllers to counteract the nonlinearity (e.g. Di Meglio et al. (2010)). However, these solutions are not robust against time delays or plant/model mismatch.

An alternative approach is to identify an unstable model of the system by a closed-loop step test. We use the identified

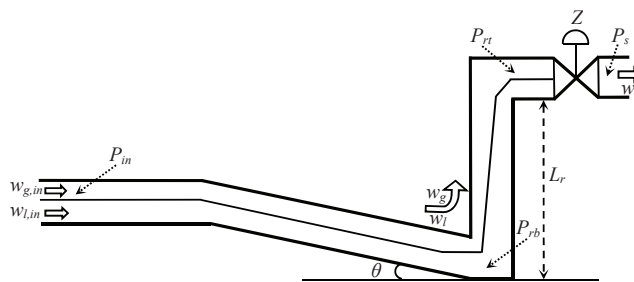


Fig. 1. Schematic presentation of system

model for an IMC (Internal Model Control) design. Then, we use the resulting IMC controller to obtain tuning parameters for PID and PI controllers.

A third approach is to use a Hammerstein model consisting of a nonlinear static gain and a linear unstable part. Based on this model, we propose simple PI tuning rules considering nonlinearity of the system.

This paper is organized as follows. An OLGA test case for simulations and our experimental setup are introduced in Section 2. Then, we present the closed-loop identification, the IMC design and the related PID/PI tunings in Section 3. A new simple model for the static nonlinear gain of the system is provided in Section 4, and simple PI tuning rules for the whole operation range are proposed in Section 5. Experimental and simulation results are shown, respectively, in Section 6 and Section 7. Finally, we summarize the main conclusions and remarks in Section 8.

2. PIPELINE-RISER SYSTEM

Fig. 1 shows a schematic presentation of the system. The inflow rates of gas and liquid to the system, $w_{g,in}$ and $w_{l,in}$, are assumed to be independent disturbances and the top-

* This work was supported by SIEMENS AS, Oil & Gas Solutions.

¹ Corresponding author

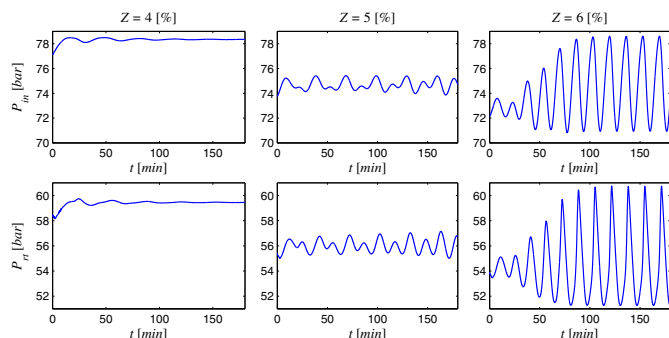


Fig. 2. Simulation results of OLGA case for different valve openings

side choke valve opening ($0 < Z < 100$) is the manipulated variable.

2.1 Olga case

As a base case, we use a test case for severe-slugging flow given in the OLGA simulator, which is a commercial multiphase simulator widely used in the oil industry. In the OLGA test case, the pipeline diameter is 0.12 m and its length is 4300 m starting from the inlet (see Fig. 1). The first 2000 m of the pipeline is horizontal and the remaining 2300 m is inclined downward with a 1° angle. The riser is a vertical 300 m pipe with a diameter of 0.1 m . Then, follows a 100 m horizontal section with the same diameter as that of the riser which connects the riser to the outlet choke valve. The feed into the system is nominally constant at 9 kg/s , with $w_{l,in} = 8.64\text{ kg/s}$ (oil) and $w_{g,in} = 0.36\text{ kg/s}$ (gas). The pressure after the choke valve P_s (separator pressure) is nominally constant at 50.1 bar .

For the present case study, the critical value of the valve opening which gives the transition between a stable non-oscillatory flow regime and a limit-cycle flow regime (riser slugging) is $Z^* = 5\%$. This is demonstrated by the OLGA simulations in Fig. 2 which show the inlet pressure and the topside pressure for the valve openings of 4% (no slug) 5% (transient) and 6% (riser slugging). Simulations, such as those in Fig. 2, were used to generate the bifurcation diagrams in Fig. 3, which show the behavior of the system over the whole working range of the choke valve (Storkaas and Skogestad (2007)). The dashed line in between represents the steady-state solution which is unstable without control for valve opening larger than 5%. For valve openings more than 5%, in addition to the steady-state solution, there are two other lines giving the maximum and minimum pressures of the persisted limit cycles (slugging flow).

2.2 Experimental setup

The experiments were performed on a laboratory setup for anti-slug control at the Chemical Engineering Department of NTNU. Fig. 4 shows a schematic presentation of the laboratory setup. The pipeline and the riser are made from flexible pipes with 2 cm inner diameter. The length of the pipeline is 4 m , and it is inclined with a 15° angle. The height of the riser is 3 m . A buffer tank is used to simulate the effect of a long pipe with the same volume, such that the total resulting length of pipe would be about 70 m .

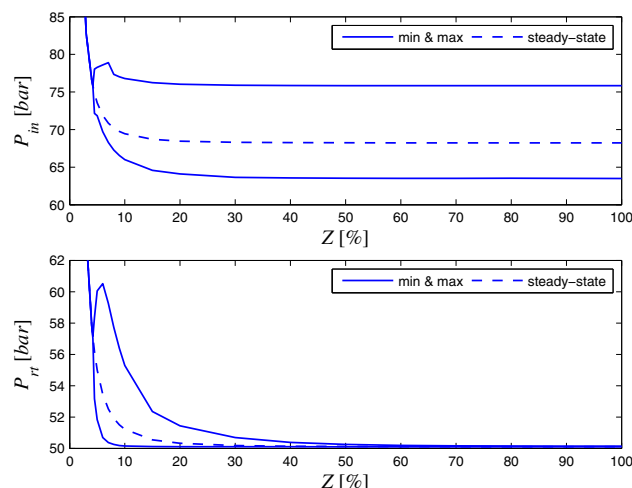


Fig. 3. Bifurcation diagrams for OLGA case

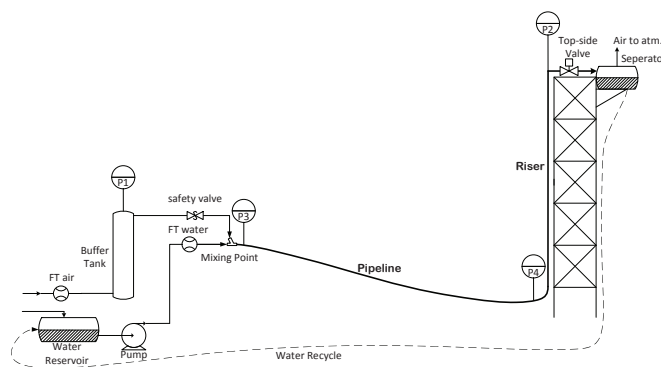


Fig. 4. Experimental setup

The topside choke valve is used as the input for control. The separator pressure after the topside choke valve is nominally constant at atmospheric pressure. The feed into the pipeline is assumed to be at constant flow rates, 4 litre/min of water and 4.5 litre/min of air. With these boundary conditions, the critical valve opening where the system switches from stable (non-slug) to oscillatory (slug) flow is at $Z^* = 15\%$ for the top-side valve. The bifurcation diagrams are shown in Fig. 5.

The desired steady-state (dashed middle line) slugging condition ($Z > 15\%$) is unstable, but it can be stabilized by using control. The slope of the steady-state line (in the middle) is the static gain of the system, $k = \partial y / \partial u = \partial P_{in} / \partial Z$. As the valve opening increase this slope decreases, and the gain finally approaches to zero. This makes control of the system with large valve openings very difficult.

3. PID/PI TUNING BASED ON IMC DESIGN

3.1 Model Identification

We use a Hammerstein model structure (Fig. 6) to describe the desired unstable operating point (flow regime). The Hammerstein model consists of series connection of a static nonlinearity and a linear time-invariant dynamic system. For our application, the static nonlinearity represents the static gain (K) of the process and $G'(s)$ accounts for

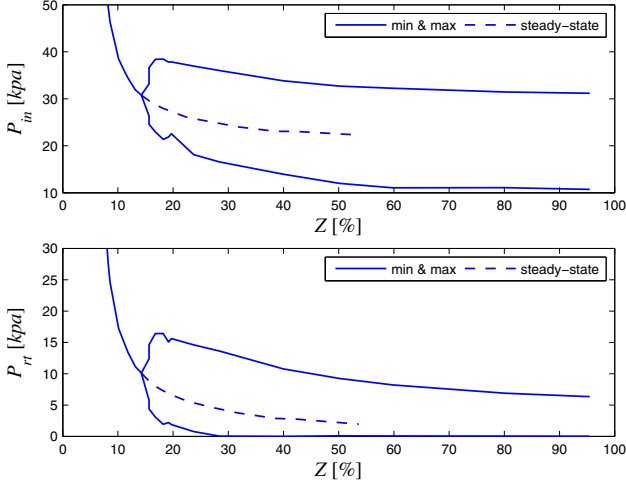


Fig. 5. Bifurcation diagrams for experimental setup

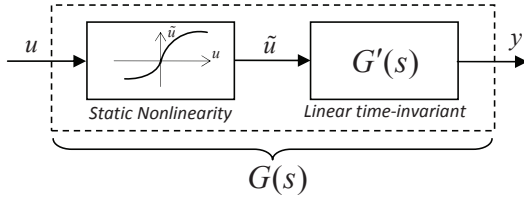


Fig. 6. Block diagram for Hammerstein model

the unstable dynamics. For identification of the unstable dynamics, we need to assume a structure. We first consider a simple unstable first-order plus dead time model:

$$G(s) = \frac{K e^{-\theta s}}{\tau s - 1} = \frac{b e^{-\theta s}}{s - a} \quad (1)$$

where $a > 0$. If we control this system with a proportional controller with the gain K_{c0} (see Fig. 7), the closed-loop transfer function from the set-point (y_s) to the output (y) becomes

$$\frac{y(s)}{y_s(s)} = \frac{K_{c0} G(s)}{1 + K_{c0} G(s)} = \frac{K_{c0} b e^{-\theta s}}{s - a + K_{c0} b e^{-\theta s}} \quad (2)$$

In order to get a stable closed-loop system, we need $K_{c0} b e^{-\theta s} > a$ and $K_{c0} b > a$. The steady-state gain of the closed-loop transfer function is

$$\frac{\Delta y_\infty}{\Delta y_s} = \frac{K_{c0} b}{K_{c0} b - a} > 1. \quad (3)$$

However, the closed-loop step response of the system in experiments, as in Fig. 8, shows that the steady-state gain of the system under study is smaller than one. Therefore, the model form in (1) is not a correct choice.

If we linearize the four-state mechanistic model by Jahan-shahi and Skogestad (2011) around the desired unstable operating point, we will get a fourth-order linear model in the form of

$$G(s) = \frac{\theta_1(s + \theta_2)(s + \theta_3)}{(s^2 - \theta_4 s + \theta_5)(s^2 + \theta_6 s + \theta_7)}. \quad (4)$$

This model contains two unstable pole, two stable poles and two zeros. Seven parameters (θ_i) must be estimated to identify this model. However, if we look at the Hankel Singular Values of the fourth order model (Fig. 9), we find that the stable part of the system has little dynamic contribution. This suggests that a model with two unstable

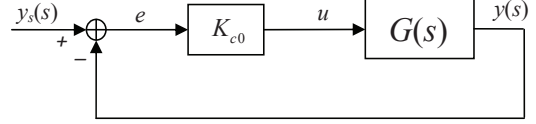


Fig. 7. Closed-loop system for step test

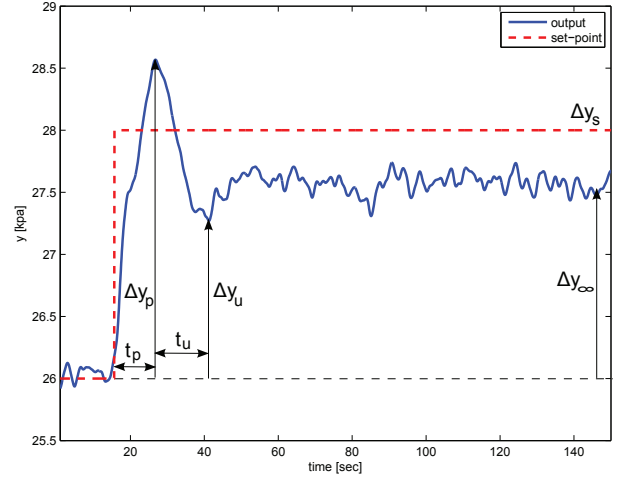


Fig. 8. Closed-loop step response for stabilized experimental system

poles is sufficient for control design. Using balanced model truncation (square root method), we obtained a reduced-order model in the form of

$$G(s) = \frac{b_1 s + b_0}{s^2 - a_1 s + a_0}, \quad (5)$$

where $a_0 > 0$ and $a_1 > 0$. The model has two unstable poles and four parameters, b_1 , b_0 , a_1 and a_0 , need to be estimated. If we control the unstable system in (5) by a proportional controller with the gain K_{c0} , the closed-loop transfer function from the set-point (y_s) to the output (y) will be

$$\frac{y(s)}{y_s(s)} = \frac{K_{c0}(b_1 s + b_0)}{s^2 + (-a_1 + K_{c0} b_1) s + (a_0 + K_{c0} b_0)}. \quad (6)$$

For the closed-loop stable system, we consider a transfer function similar to the model used by Yuwana and Seborg (1982):

$$\frac{y(s)}{y_s(s)} = \frac{K_2(1 + \tau_2 s)}{\tau^2 s^2 + 2\zeta\tau s + 1} \quad (7)$$

We use six data (Δy_p , Δy_u , Δy_∞ , Δy_s , t_p and t_u) observed from the closed-loop response (see Fig. 8) to estimate the four parameters (K_2 , τ_z , τ and ζ) in (7). Then, we back-calculate the parameters of the open-loop unstable model in (5). Details are given in Appendix A.

3.2 IMC design for unstable systems

Internal Model Control (IMC) is summarized by Morari and Zafriou (1989). The block diagram of the IMC structure is shown in Fig. 10. Where $G(s)$ is model of the plant which in general has some mismatch with the real plant $G_p(s)$. $\hat{Q}(s)$ is the inverse of the minimum phase part of $G(s)$ and $f(s)$ is a low-pass filter for robustness of the closed-loop system. The IMC configuration cannot be

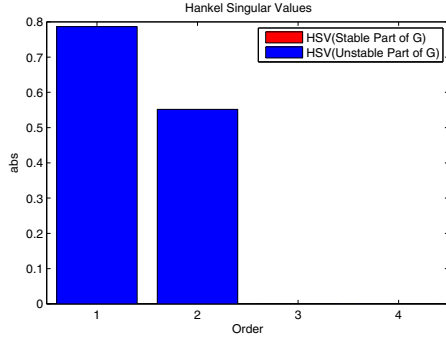


Fig. 9. Hankel Singular Values of fourth order model

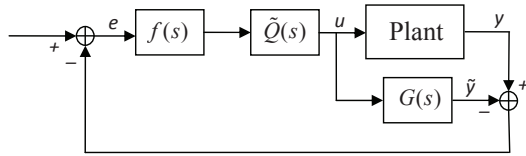


Fig. 10. Block diagram of Internal Model Control system used directly for unstable systems; instead the stabilizing controller is given as

$$C(s) = \frac{\tilde{Q}(s)f(s)}{1 - G(s)\tilde{Q}(s)f(s)} \quad (8)$$

For internal stability, $\tilde{Q}f$ and $(1 - G\tilde{Q}f)$ have to be stable. We use the identified model in the previous section as the plant model:

$$G(s) = \frac{\hat{b}_1 s + \hat{b}_0}{s^2 - \hat{a}_1 s + \hat{a}_0} = \frac{k'(s + \varphi)}{(s - \pi_1)(s - \pi_2)} \quad (9)$$

and we get

$$\tilde{Q}(s) = \frac{(1/k')(s - \pi_1)(s - \pi_2)}{s + \varphi} \quad (10)$$

We design the filter $f(s)$ as explained by Morari and Zafiriou (1989):

$k = \text{number of RHP poles} + 1 = 3$

$m = \text{max}(\text{number of zeros of } \tilde{Q}(s) - \text{number of pole of } \tilde{Q}(s), 1) = 1$ (this is for making $Q = \tilde{Q}f$ proper)

$n = m + k - 1 = 3$; filter order

The filter is in the following from:

$$f(s) = \frac{\alpha_2 s^2 + \alpha_1 s + \alpha_0}{(\lambda s + 1)^3}, \quad (11)$$

Where λ is an adjustable filter time-constant. We choose $\alpha_0 = 1$ to get an integral action and the coefficients α_1 and α_2 are calculated by solving the following system of linear equations:

$$\begin{pmatrix} \pi_1^2 & \pi_1 & 1 \\ \pi_2^2 & \pi_2 & 1 \end{pmatrix} \begin{pmatrix} \alpha_2 \\ \alpha_1 \\ \alpha_0 \end{pmatrix} = \begin{pmatrix} (\lambda\pi_1 + 1)^3 \\ (\lambda\pi_2 + 1)^3 \end{pmatrix} \quad (12)$$

The feedback version of the IMC controller becomes

$$C(s) = \frac{[\frac{1}{k'\lambda^3}](\alpha_2 s^2 + \alpha_1 s + 1)}{s(s + \varphi)} \quad (13)$$

3.3 PID-F tuning rules

The IMC controller in (13) is a second order transfer function which can be written in form of a PID controller

with a low-pass filter.

$$K_{PID}(s) = K_c + \frac{K_i}{s} + \frac{K_d s}{T_f s + 1} \quad (14)$$

Where

$$T_f = 1/\varphi \quad (15)$$

$$K_i = \frac{T_f}{k'\lambda^3} \quad (16)$$

$$K_c = K_i \alpha_1 - K_i T_f \quad (17)$$

$$K_d = K_i \alpha_2 - K_c T_f \quad (18)$$

We require $K_c < 0$ and $K_d < 0$, in order that the controller works in practice. We must choose λ such that these two conditions are satisfied.

3.4 PI tuning rules

For a PI controller in the following form

$$K_{PI}(s) = K_c \left(1 + \frac{1}{\tau_I s} \right), \quad (19)$$

the tuning rules are derived from the controller (13) as follows

$$K_c = \lim_{s \rightarrow \infty} C(s) = \frac{\alpha_2}{k'\lambda^3} \quad (20)$$

$$\tau_I = \frac{K_c}{\lim_{s \rightarrow 0} sC(s)} = \alpha_2 \varphi \quad (21)$$

This means that the PI-controller approximates high-frequency and low-frequency asymptotes of $C(s)$ in (13).

4. SIMPLE MODEL FOR STATIC NONLINEARITY

So far, we have used experimental work to obtain the model. However, we can estimate the static gain. The slope of the steady-state line in Fig. 3 is the static gain of the system which is related to valve properties. We assume the valve equation as the following:

$$w = C_v f(z) \sqrt{\rho \Delta P} \quad (22)$$

where $w[kg/s]$ is the outlet mass flow and $\Delta P[N/m^2]$ is the pressure drop. From the valve equation, the pressure drop over the valve for different valve openings can be written as

$$\Delta P = \frac{\bar{a}}{f(z)^2}, \quad (23)$$

where we assume \bar{a} as a constant parameter calculated in Appendix B. Our simple empirical model for the inlet pressure is as follows:

$$P_{in} = \frac{\bar{a}}{f(z)^2} + \bar{P}_{fo} \quad (24)$$

Where \bar{P}_{fo} is another constant parameter that is the inlet pressure when the valve is fully open, and it is given in Appendix B. By differentiating (24) with respect to z , we get the static gain of the system as a function of valve opening.

$$k(z) = \frac{-2\bar{a} \frac{\partial f(z)}{f(z)^3}}{f(z)^3} \quad (25)$$

For a linear valve (i.e. $f(z) = z$) it reduces to

$$k(z) = \frac{-2\bar{a}}{z^3}, \quad (26)$$

where $0 \leq z \leq 1$. Fig. 11 compares the simple static model in (24) and (25) to the Olga model.

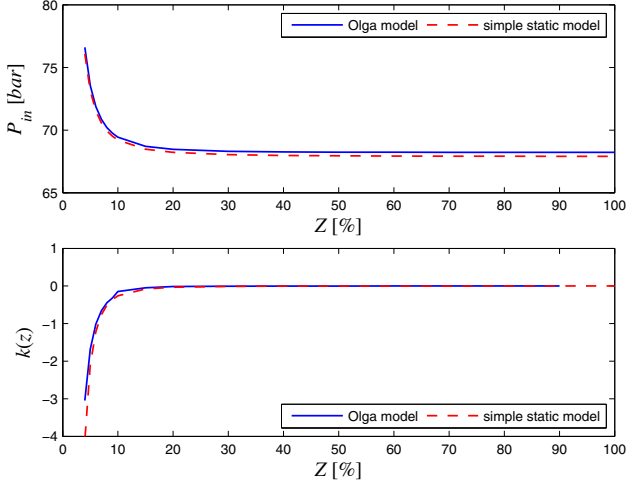


Fig. 11. Simple static model compared to OLGA case

5. PI TUNING CONSIDERING NONLINEARITY

The PID and PI tuning rules given in above are based on a linear model identified at a certain operating point. However, as we see in Fig. 11, the gain of the system changes drastically with the valve opening. Hence, a controller working at one operating point may not work at other operating points.

One solution is gain-scheduling with multiple controllers based on multiple identified modes. We propose simple PI tuning rules based on single step test, but with a gain correction to counteract the nonlinearity of the system. For this, we use the static model given in (25). We perform a closed-loop step test and we use the data in Fig. 8 to calculate

$$\beta = \frac{-\ln\left(\frac{\Delta y_\infty - \Delta y_u}{\Delta y_p - \Delta y_\infty}\right)}{2\Delta t} + \frac{K_{c0}k(z_0)\left(\frac{\Delta y_p - \Delta y_\infty}{\Delta y_\infty}\right)^2}{4t_p}, \quad (27)$$

where z_0 is the average valve opening in the closed-loop step test and K_{c0} is the proportional gain used for the test. The PI tuning values as functions of valve opening are given as the following:

$$K_c(z) = \frac{\beta T_{osc}}{k(z)\sqrt{z/z^*}} \quad (28)$$

$$\tau_I(z) = 3T_{osc}(z/z^*) \quad (29)$$

Where T_{osc} is the period of slugging oscillations when the system is open-loop and z^* is the critical valve opening of the system (at the bifurcation point).

6. EXPERIMENTAL RESULTS

6.1 Experiment 1: PID and PI tuning at $Z=20\%$

The system switches to slugging flow at 15% of valve opening, hence it is unstable at 20%. We closed the loop by a proportional controller $K_{c0} = -10$ and changed the set-point by 2 kPa (Fig. 12). Since the response is noisy, a low-pass filter was used to reduce the noise effect. Then, we use the method explained in Section 3.1 to identify the closed-loop stable system as the following:

$$\frac{y(s)}{y_s(s)} = \frac{2.317s + 0.8241}{19.91s^2 + 2.279s + 1} \quad (30)$$

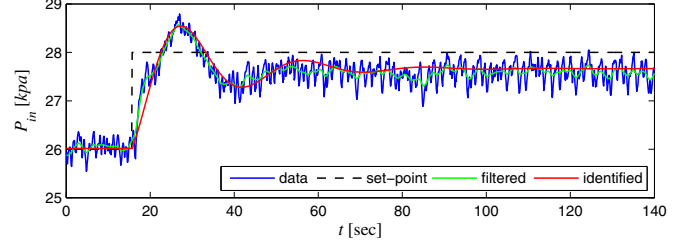


Fig. 12. Closed-loop step test for experiment 1

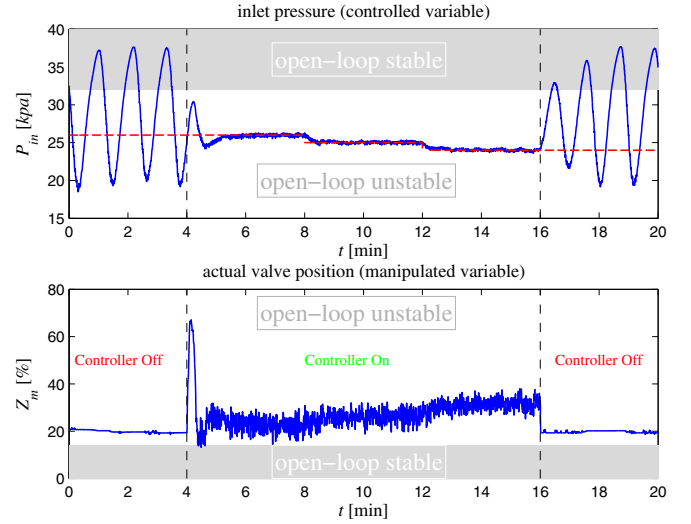


Fig. 13. Result of PID controller for experiment 1

The identified closed-loop transfer function is shown by the red line in Fig. 12. Then, we back calculate to the open-loop unstable system:

$$G(s) = \frac{-0.012s - 0.0041}{s^2 - 0.0019s + 0.0088} \quad (31)$$

We select $\lambda = 10$ for an IMC design to get the controller:

$$C(s) = \frac{-25.94(s^2 + 0.07s + 0.0033)}{s(s + 0.35)} \quad (32)$$

The related PID tuning values, as in Section 3.3, are $K_c = -4.44$, $K_i = -0.24$, $K_d = -60.49$ and $T_f = 2.81$. Fig. 13 shows result of control using the PID controller. This controller was tuned for 20% valve opening, but it can stabilize the system up to 32% valve opening which shows good gain margin of the controller. In addition, we tested its delay margin by adding time-delay to the measurement. It was stable with 3 sec added time delay.

The related PI tuning values, as in Section 3.4, are $K_c = -25.95$ and $\tau_I = 107.38$. Fig. 14 shows result of experiment using the PI controller. This controller was stable with 2 sec time-delay.

6.2 Experiment 2: PID and PI tuning at $Z=30\%$

We repeated the previous experiment at 30% valve opening. We closed the loop by a proportional controller $K_{c0} = -20$ and changed the set-point by 2 kPa (Fig. 15). Then, we use the method explained in Section 3.1 to identify the closed-loop stable system as the following:

$$\frac{y(s)}{y_s(s)} = \frac{2.634s + 0.6635}{13.39s^2 + 2.097s + 1} \quad (33)$$

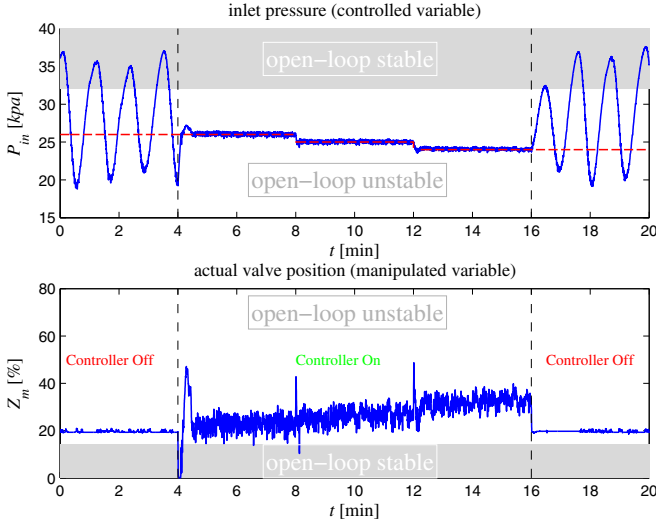


Fig. 14. Result of PI controller for experiment 1

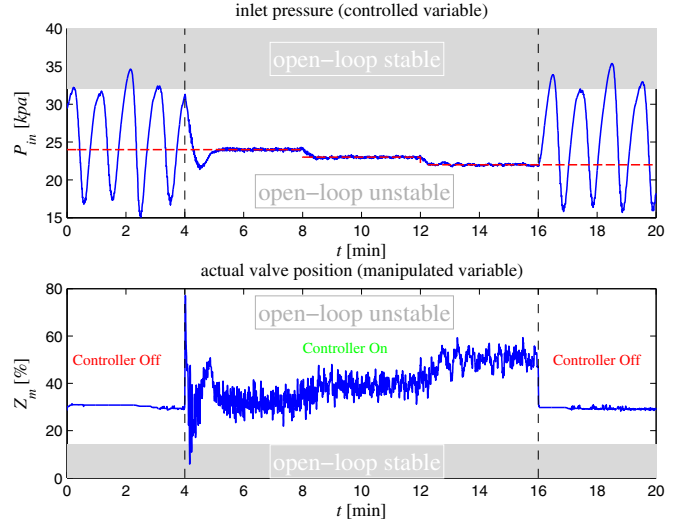


Fig. 16. Result of PID controller for experiment 2

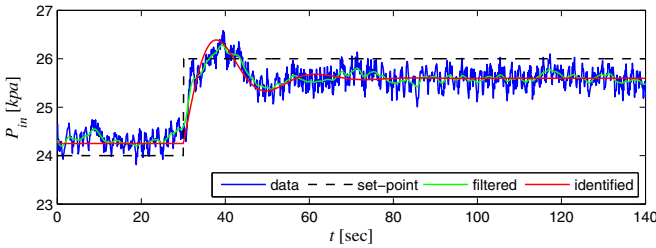


Fig. 15. Closed-loop step test for experiment 2

The identified closed-loop transfer function is shown by the red line in Fig. 15. Then, we back calculate to the open-loop unstable system:

$$G(s) = \frac{-0.0098s - 0.0025}{s^2 - 0.0401s + 0.0251} \quad (34)$$

We select $\lambda = 8$ for an IMC design to get the controller:

$$C(s) = \frac{-42.20(s^2 + 0.052s + 0.0047)}{s(s + 0.251)} \quad (35)$$

The related PID tuning values, as in Section 3.3, are $K_c = -5.65$, $K_i = -0.79$, $K_d = -145.15$ and $T_f = 3.97$. Fig. 16 shows result of control using the PID controller. This controller was tuned for 30% valve opening, but it can stabilize the system up to 50% valve opening which shows good gain margin of the controller. In addition, we tested its delay margin by adding time-delay to the measurement. It was stable with 2 sec added time delay.

The related PI tuning values, as in Section 3.4, are $K_c = -42.20$ and $\tau_I = 53.53$. Fig. 17 shows result of experiment using the PI controller. This controller was stable only with less than 1 sec time-delay.

6.3 Experiment 3: Adaptive PI tuning

We calculated $\beta = 0.061$ from (27) using the step test information of *Experiment 1* (Fig. 12) and the period of the slugging oscillations $T_{osc} = 68$ sec. We used the PI tuning given in (28) and (29) in an adaptive manner to control the system. The valve opening has many variations and it cannot be used directly; a low-pass filter was used to make it smooth. The result of control using this tuning is

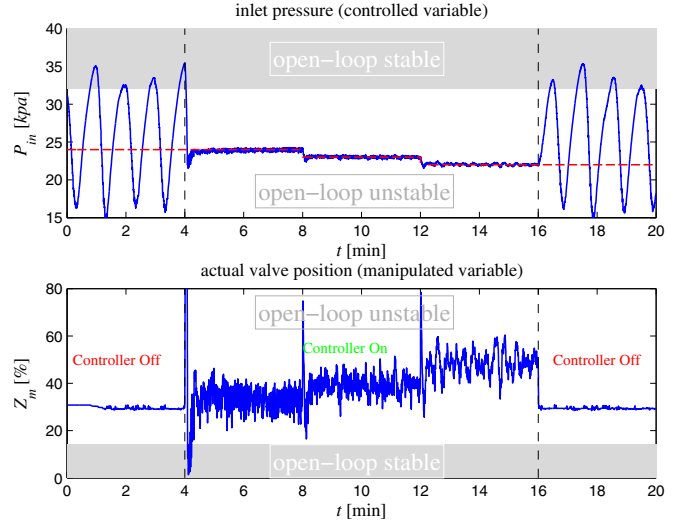


Fig. 17. Result of PI controller for experiment 2

shown in Fig. 18. The controller gains are given in Fig. 19. This simple adaptive controller could stabilize the system from 20% to 50%, and it was stable even with 1sec added time delay.

7. OLGA SIMULATION

We tested the PI tuning rules in (28) and (29) on the Olga case presented in Section 2.1. The PI tuning values are given in Table 1 and the simulation result is shown in Fig. 20. The open-loop system switches to slugging flow at 5% valve opening (Fig. 2), but by using the proposed PI tuning the system could be stabilized up to 23.24% valve opening.

8. CONCLUSION

A model structure including two unstable poles and one zero was used to identify an unstable model for slugging flow dynamics. The model parameters were estimated from a closed-loop step test (step change in the set-point of the controller). The identified model was used for an IMC

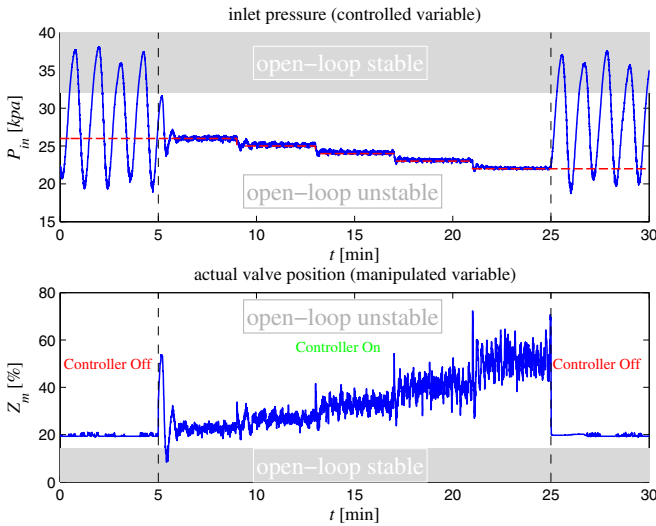


Fig. 18. Result of control using adaptive PI tuning in experiment 3

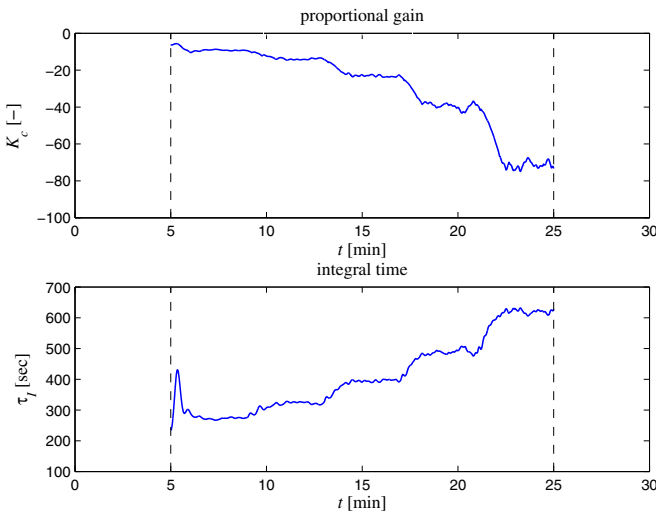


Fig. 19. Controller gains resulted from adaptive PI tuning in experiment 3

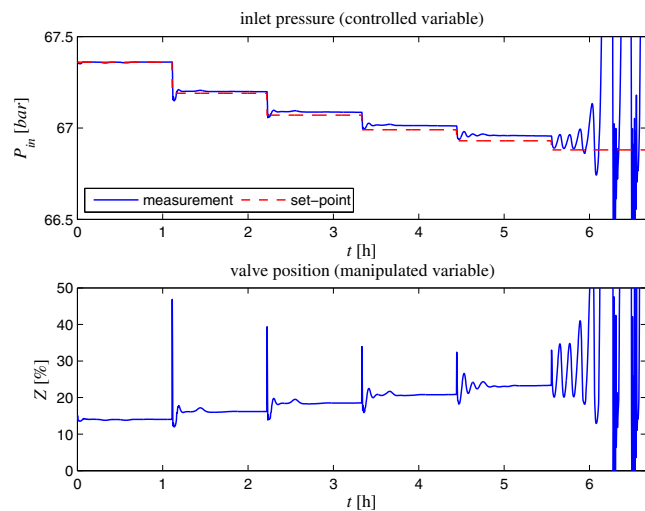


Fig. 20. Result of control from Olga simulation

design, then PID and PI tunings were obtained from the resulted IMC controller. This scheme was tested in experiments which shows applicability and robustness of the method. A PID controller with the proposed tuning was identical to the IMC that retains good phase-margin and gain-margin.

Moreover, a simple static model was introduced to account for the intense nonlinearity in static gain of the system, then a one-step PI tuning was proposed based on the static model. This method could stabilize the system on a wide range of valve opening in both experiments and Olga simulations.

REFERENCES

- Di Meglio, F., Kaasa, G.O., Petit, N., and Alstad, V. (2010). Model-based control of slugging flow: an experimental case study. In *American Control Conference*. Baltimore, USA.
- Godhavn, J.M., Fard, M.P., and Fuchs, P.H. (2005). New slug control strategies, tuning rules and experimental results. *Journal of Process Control*, 15, 547557.
- Havre, K., Stornes, K., and Stray, H. (2000). Taming slug flow in pipelines. *ABB Review*, (4), 55–63.
- Jahanshahi, E. and Skogestad, S. (2011). Simplified dynamical models for control of severe slugging in multi-phase risers. In *18th IFAC World Congress*, 1634–1639. Milan, Italy.
- Morari, M. and Zafriou, E. (1989). *Robust Process Control*. Prentice Hall, Englewood Cliffs, New Jersey.
- Storkaas, E. and Skogestad, S. (2007). Controllability analysis of two-phase pipeline-riser systems at riser slugging conditions. *Control Engineering Practice*, 15(5), 567–581.
- Taitel, Y. (1986). Stability of severe slugging. *International Journal of Multiphase Flow*, 12(2), 203–217.
- Yuwana, M. and Seborg, D.E. (1982). A new method for on-line controller tuning. *AIChE Journal*, 28(3), 434–440.

Appendix A. MODEL IDENTIFICATION CALCULATIONS

Stable closed-loop transfer function:

$$\frac{y(s)}{y_s(s)} = \frac{K_2(1 + \tau_2 s)}{\tau^2 s^2 + 2\zeta\tau s + 1} \quad (\text{A.1})$$

The Laplace inverse (time-domain) of the transfer function in (A.1) is (Yuwana and Seborg (1982))

$$y(t) = \Delta y_s K_2 [1 + D \exp(-\zeta t/\tau) \sin(Et + \phi)], \quad (\text{A.2})$$

where

$$D = \frac{\left[1 - \frac{2\zeta\tau_2}{\tau} + \left(\frac{\tau_2}{\tau}\right)^2\right]^{\frac{1}{2}}}{\sqrt{1 - \zeta^2}} \quad (\text{A.3})$$

Table 1. PI tuning values in Olga simulation

set-point	valve opening	K_c	τ_I
67.36	14	0.5	8400
67.19	16.1	0.7	9600
67.07	18.2	0.94	10800
66.99	20.1	1.23	12000
66.93	23.24	1.56	13200
66.88	–	1.93	14400

$$E = \frac{\sqrt{1-\zeta^2}}{\tau} \quad (\text{A.4})$$

$$\phi = \tan^{-1} \left[\frac{\tau\sqrt{1-\zeta^2}}{\zeta\tau - \tau_z} \right] \quad (\text{A.5})$$

By differentiating (A.2) with respect to time and setting the derivative equation to zero, one gets time of the first peak:

$$t_p = \frac{\tan^{-1} \left(\frac{1-\zeta^2}{\zeta} \right) + \pi - \phi}{\sqrt{1-\zeta^2}/\tau} \quad (\text{A.6})$$

And the time between the first peak (overshoot) and the undershoot:

$$t_u = \pi\tau/\sqrt{1-\zeta^2} \quad (\text{A.7})$$

The damping ratio ζ can be estimated as

$$\hat{\zeta} = \frac{-\ln v}{\sqrt{\pi^2 + (\ln v)^2}} \quad (\text{A.8})$$

where

$$v = \frac{\Delta y_\infty - \Delta y_u}{\Delta y_p - \Delta y_\infty} \quad (\text{A.9})$$

Then, using equation (A.7) we get

$$\hat{\tau} = \frac{t_u\sqrt{1-\hat{\zeta}^2}}{\pi}. \quad (\text{A.10})$$

The steady-state gain of the closed-loop system is estimated as

$$\hat{K}_2 = \frac{\Delta y_\infty}{\Delta y_s}. \quad (\text{A.11})$$

We use time of the peak t_p and (A.6) to get an estimate of ϕ :

$$\hat{\phi} = \tan^{-1} \left[\frac{1-\hat{\zeta}^2}{\hat{\zeta}} \right] - \frac{t_p\sqrt{1-\hat{\zeta}^2}}{\hat{\tau}} \quad (\text{A.12})$$

From (A.4), we get

$$\hat{E} = \frac{\sqrt{1-\hat{\zeta}^2}}{\hat{\tau}} \quad (\text{A.13})$$

The overshoot is defined as

$$D_0 = \frac{\Delta y_p - \Delta y_\infty}{\Delta y_\infty}. \quad (\text{A.14})$$

By evaluating (A.2) at time of peak t_p we get

$$\Delta y_p = \Delta y_s \hat{K}_2 \left[1 + \hat{D} \exp(-\hat{\zeta}t_p/\hat{\tau}) \sin(\hat{E}t_p + \hat{\phi}) \right] \quad (\text{A.15})$$

Combining equation (A.11), (A.14) and (A.15) gives

$$\hat{D} = \frac{D_0}{\exp(-\hat{\zeta}t_p/\hat{\tau}) \sin(\hat{E}t_p + \hat{\phi})}. \quad (\text{A.16})$$

We can estimate the last parameter by solving (A.3):

$$\hat{\tau}_z = \hat{\xi}\hat{\tau} + \sqrt{\hat{\zeta}^2\hat{\tau}^2 - \hat{\tau}^2 \left[1 - \hat{D}^2(1-\hat{\zeta}^2) \right]} \quad (\text{A.17})$$

Then, we back-calculate to parameters of the open-loop unstable model. The steady-state gain of the open-loop model is

$$\hat{K} = \frac{\Delta y_\infty}{K_{c0} |\Delta y_s - \Delta y_\infty|} \quad (\text{A.18})$$

From this, we can estimate the four model parameters in equation (5) are

$$\hat{a}_0 = \frac{1}{\hat{\tau}^2(1 + K_{c0}\hat{K}_p)} \quad (\text{A.19})$$

$$\hat{b}_0 = \hat{K}_p\hat{a}_0 \quad (\text{A.20})$$

$$\hat{b}_1 = \frac{\hat{K}_2\hat{\tau}_z}{K_{c0}\hat{\tau}^2} \quad (\text{A.21})$$

$$\hat{a}_1 = -2\hat{\zeta}/\hat{\tau} + K_{c0}\hat{b}_1, \quad (\text{A.22})$$

where $\hat{a}_1 > 0$ gives an unstable system.

Appendix B. CALCULATION OF STATIC NONLINEARITY PARAMETERS

From equation (22) we have

$$\bar{a} = \frac{1}{\bar{\rho}} \left(\frac{\bar{w}}{C_v} \right)^2 \quad (\text{B.1})$$

Where C_v is the known valve constant, \bar{w} is the steady-state average outlet flow rate and $\bar{\rho}$ is the steady-state average mixture density. The average outlet mass flow is approximated by constant inflow rates.

$$\bar{w} = w_{g,in} + w_{l,in} \quad (\text{B.2})$$

In order to estimate the average mixture density $\bar{\rho}$, we perform the following calculations, assuming a fully open valve.

Average gas mass fraction:

$$\bar{\alpha} = \frac{w_{g,in}}{w_{g,in} + w_{l,in}} \quad (\text{B.3})$$

Average gas density at top of the riser from ideal gas law:

$$\bar{\rho}_g = \frac{(P_s + \Delta P_{v,\min})M_g}{RT} \quad (\text{B.4})$$

where P_s is the constant separator pressure, and $\Delta P_{v,\min}$ is the (minimum) pressure drop across the valve that exists with a fully open valve. In the numerical simulations $\Delta P_{v,\min}$ is assumed to be zero but in our experiments it was 2 kPa.

Liquid volume fraction:

$$\bar{\alpha}_l = \frac{(1-\bar{\alpha})\bar{\rho}_g}{(1-\bar{\alpha})\bar{\rho}_g + \bar{\alpha}\rho_L}. \quad (\text{B.5})$$

Average mixture density:

$$\bar{\rho} = \bar{\alpha}_l\rho_l + (1-\bar{\alpha}_l)\bar{\rho}_g \quad (\text{B.6})$$

In order to calculate the constant parameters \bar{P}_{fo} in (24), we use the fact that if the inlet pressure is large enough to overcome a riser full of liquid, slugging will not happen. Taitel (1986) used the same concept for stability analysis, also this was observed in our experiments. we define the critical pressure as

$$P_{in}^* = \rho_L g L_r + P_s + \Delta P_{v,\min} \quad (\text{B.7})$$

This pressure is associated with the critical valve opening at the bifurcation point z^* . From (24), we get \bar{P}_{fo} as the following:

$$\bar{P}_{fo} = P_{in}^* - \frac{\bar{a}}{f(z^*)^2} \quad (\text{B.8})$$